

Electronic structure of Pd₃Fe: Ordered phase

C. A. Kuhnen* and E. Z. da Silva

Instituto de Física Gleb Wataghin, Universidade Estadual de Campinas, Campinas São Paulo, Brazil

(Received 18 March 1986; revised manuscript received 28 July 1986)

The electronic structure of Pd₃Fe is studied using the self-consistent linear-muffin-tin orbital method. We consider first the paramagnetic phase of Pd₃Fe, discussing its instability with respect to the formation of the ferromagnetic state, and proceed to calculate its ferromagnetic phase. Results concerning the magnetization and the linear coefficient of the specific heat compare well with available experiments in the spin-polarized case. Together with bands along symmetry directions and densities of states we also offer a discussion of the Fermi surface of ferromagnetic Pd₃Fe.

I. INTRODUCTION

Alloys of Pd-Fe have a continuous range of solid solubility which includes several compounds. Some of the compounds can be prepared in various degrees of order, from completely disordered to totally ordered phases. One of these compounds, Pd₃Fe, has been the object of many experimental studies of thermal properties,¹ magnetic properties,²⁻⁶ as well as hydrogenation,⁷ both in ordered and disordered states.

Pd₃Fe in the ordered phase has a Cu₃Au structure, which is a fcc lattice, with Fe atoms located in the corners and Pd atoms at its face centers. The disordered phase of Pd₃Fe is a fcc structure where the sites can be randomly occupied by Pd or Fe atoms with concentrations $c=0.75$ and $1-c=0.25$, respectively. The experimental lattice parameter for this compound in both phases is $a=3.849$ Å, which is used in the present calculation. Pd₃Fe presents many features of interest due to its unusual properties. Although metallic Pd is paramagnetic, small quantities of Fe make the ferromagnetic ground state of these alloys stable. In particular Pd₃Fe is ferromagnetic in both the ordered and disordered phases with a Curie temperature for the ordered compound of $T=499$ K.³ Despite its cubic symmetry, one interesting feature of this alloy is the considerable anisotropy in the spin-wave dispersion, observed by Stirling *et al.*² This observed anisotropy cannot be explained either by a localized magnetic model or by an itinerant one, but a mixed model proposed by Yamada and Shimizu,⁸ seems capable of explaining this behavior. However, this shows the need for a reliable band-structure calculation for this alloy which may help us decide the mechanisms responsible for the unusual behavior of this system, as well as allowing us to compare theory with other experimental data.

The Mössbauer effect was used by Tsurin and Men'shikov⁴ to measure the local magnetic moments in Pd and Fe sites, both in ordered and disordered phases of the alloy. In ordered Pd₃Fe the magnetic moments at Pd and Fe sites were $0.57\mu_B$ and $2.70\mu_B$, respectively. The transition to a disordered phase raised the value of the magnetic moment on the Fe site to $3.00\mu_B$, and lowered the value on the Pd site to $0.34\mu_B$. Specific-heat measurements were performed by Bechman *et al.*¹ The linear

coefficient of the electronic specific heat for this alloy in the ordered and disordered phases was found to be $\gamma=8.17$ mJ/mol K² for the ordered Pd₃Fe, which corresponds to 0.867 states/eV atom for the density of states at the Fermi level. For the disordered state they found $\gamma=11.28$ mJ/mol K², which gives 1.196 states/eV atom at the Fermi level. Pd₃Fe is also an important material due to its capacity to absorb large amounts of hydrogen in its ordered phase. Our present calculation does not deal with hydrogen absorption, but can be viewed as a reference calculation if one is going to study hydrogen absorption. We shall return to the question of Pd₃Fe hydrides in a future publication.

In this work we study the electronic structure of ferromagnetic Pd₃Fe alloy. The local magnetic moments obtained agree well with experimental data as well as other theoretical semi-empirical results obtained using the Bethe lattice approximation.⁹ In general, the method employed gives good results as we shall describe. In the next section we describe briefly some specific details of the method used in the present calculation. In Sec. III we present, first, a brief discussion of the paramagnetic calculation of the alloy, then present the results for the ferromagnetic compound in terms of the band structure, state density and cross sections of the Fermi surface, along the high-symmetry planes of the Brillouin zone, for the up- and down-spin bands. Finally, in Sec. IV, we present the main conclusions of this work, and we argue the necessity of an electronic structure calculation of the alloy in the disordered state, for a clear understanding of the influence of order in the behavior of Pd₃Fe.

II. METHOD OF CALCULATION

The framework of the density-functional theory of Hohenberg, Kohn, and Sham^{10,11} gives a prescription for obtaining self-consistent electronic potentials for solids. In particular we apply the local approximation of Hedin and Lundqvist¹² to the density-functional theory for the paramagnetic calculations and the von Barth and Hedin¹³ approximation to the spin-density functional theory for the magnetic calculations. We use the linear muffin-tin-orbital method (LMTO) of Andersen,¹⁴ which combines the idea of the LCAO (linear combination of atomic orbi-

tals) method with the most desirable properties of the Korringa-Kohn-Rostoker (KKR) method.^{15,16} Like KKR, the LMTO method has the capability of treating both simple and *d*-band metals,^{17,18} with the advantage of being much faster computationally since its secular equations are of the LCAO form, and therefore eigenvalues and eigenvectors for a given Bloch vector, may be obtained by a single diagonalization.¹⁴ Within the atomic-sphere approximation (ASA), the secular equation of the LMTO method is separated into two distinct parts, one of which depends only on the crystal structure and is expressed in terms of canonical bands which have a complicated dependence on the *k* wave vector. The other part of the secular equation depends only on the crystal potential and on the volume of the atomic spheres and is expressed in terms of the potential parameters, which convert the canonical bands into energy bands by specifying their positions and widths on the energy scale. Since the LMTO method has been described in great detail in many publications (see, for example, Skriver's book¹⁹) we shall limit ourselves to a description of particular details of the present calculation. We have used the self-consistent LMTO method with no spin-orbit interaction, and the combined correction terms were not included. The spheres around the atoms were taken to be of equal size, and their values were $S=2.843$ a.u. For this choice our results for the converged SCF potentials and charges showed very small charge transfer. The excess charge at Fe atoms in the ferromagnetic calculation was $0.0169e$. The one-electron potentials were self-consistently obtained with 165 *k* points for the paramagnetic and 220 *k* points for the ferromagnetic calculation, using the tetrahedron method.²⁰

III. RESULTS

A. Pd₃Fe: Paramagnetic calculation

Our first calculations are for Pd₃Fe in its paramagnetic phase. As a starting point we used the charge densities and the potentials of pure Pd and Fe crystals, also obtained using the SCF-LMTO method.²¹ The results of the self-consistent calculation for paramagnetic Pd₃Fe are shown in Table I. A comparison of these parameters for Pd and Fe in the compound with those of the pure Pd and Fe, shown in parentheses in Table I indicate that, in going from the pure constituent metals to the ordered Pd₃Fe, subtle alterations occur in the boundary conditions for the crystalline potential at each site, in such way that no drastic alterations are observed. In our calculation we observed a tendency to form Pd₃Fe originating in the change in the calculated cohesive energies from the pure Pd and Fe crystals²¹ to the calculated cohesive energy of Pd₃Fe.

We present in Fig. 1 the total density of states (DOS) for the Pd₃Fe and the *d*-projected DOS at Pd and Fe sites, obtained using the parameters of Table I. We have used 165 *k* points in the irreducible Brillouin zone (the same number of points used to achieve self-consistency). We see in Fig. 1 that the density of states at the Fermi energy E_F have a peak which is due to both Fe and Pd contributions in the projected DOS. For states below E_F the DOS

TABLE I. Potential parameters for the ordered paramagnetic Pd₃Fe. Muffin-tin radius $S=2.843$ atomic units. In parentheses are shown the potentials parameters for pure Pd ($S=2.873$ a.u.) and for pure Fe ($S=2.662$ a.u.), both in a fcc lattice.

| | | Pd | Fe |
|---------------------------------------|----------|-----------------|-----------------|
| E_v (Ry) | <i>s</i> | -0.500 (-0.435) | -0.508 (-0.421) |
| | <i>p</i> | -0.364 (-0.239) | -0.398 (-0.243) |
| | <i>d</i> | -0.350 (-0.328) | -0.239 (-0.135) |
| W (-)(Ry) | <i>s</i> | 0.159 (0.080) | 0.153 (0.165) |
| | <i>p</i> | 1.036 (0.863) | 0.938 (1.007) |
| | <i>d</i> | 0.019 (-0.011) | 0.044 (0.047) |
| $10S\Phi_{(-)}^2$ (Ry) | <i>s</i> | 3.323 (3.217) | 3.119 (3.765) |
| | <i>p</i> | 3.237 (3.086) | 2.952 (3.462) |
| | <i>d</i> | 0.358 (0.342) | 0.221 (0.302) |
| Φ_{-}/Φ_{+} | <i>s</i> | 0.862 (0.857) | 0.854 (0.859) |
| | <i>p</i> | 0.708 (0.696) | 0.686 (0.689) |
| | <i>d</i> | 0.068 (0.047) | -0.011 (-0.013) |
| $\langle \phi_v^2 \rangle^{1/2}$ (Ry) | <i>s</i> | 4.630 (4.367) | 4.115 (5.076) |
| | <i>p</i> | 6.410 (5.988) | 5.650 (6.536) |
| | <i>d</i> | 0.963 (0.910) | 0.653 (0.811) |

is mainly due to the Pd contribution while the Fe contribution is mainly manifested around and above E_F . The density of states at the Fermi level is $N(E_F)=154.7$ states/unit cell Ry, which gives a much too high coefficient to the linear specific heat, $\gamma=26.4$ mJ/mol K. This high value of $N(E_F)$ shows using the Stoner criterium

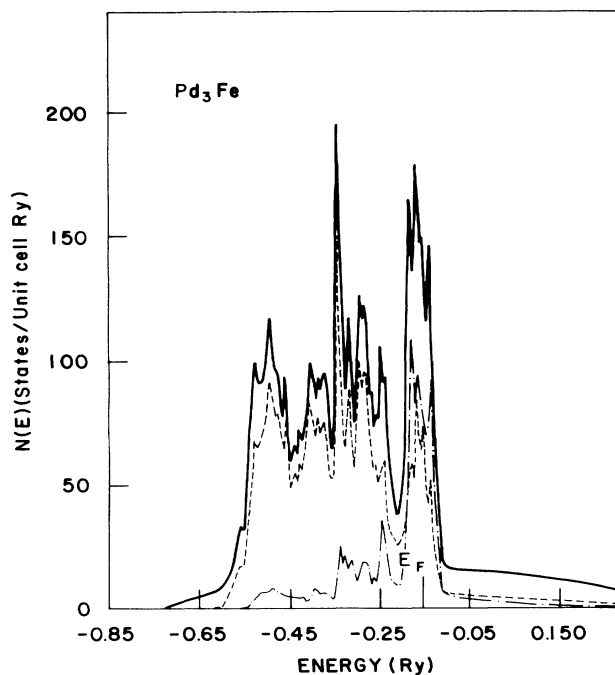


FIG. 1. The total density of states $N(E)$ (in states/unit-cell Ry) for the ordered Pd₃Fe alloy in the paramagnetic state and *d*-projected DOS (in states/atom Ry) at Pd (dashed line) and Fe (dashed-dotted line) sites. For the Pd site the *d* contribution is shown for three Pd atoms.

TABLE II. Potential parameters for the ordered spin polarized Pd₃Fe. $S=2.843$ a.u.

| | | Pd | | Fe | |
|----------------------------------------|-----|--------|--------|--------|--------|
| | | ↓ | ↑ | ↓ | ↑ |
| E_v (Ry) | s | -0.488 | -0.502 | -0.498 | -0.521 |
| | p | -0.348 | -0.380 | -0.386 | -0.393 |
| | d | -0.339 | -0.335 | -0.280 | -0.311 |
| $W(-)$ (Ry) | s | 0.156 | 0.166 | 0.149 | 0.126 |
| | p | 1.027 | 1.058 | 0.933 | 0.890 |
| | d | 0.030 | 0.010 | 0.133 | 0.002 |
| $10S\Phi_{(-)}^2$ (Ry) | s | 3.332 | 3.324 | 3.140 | 3.073 |
| | p | 3.240 | 3.247 | 2.965 | 2.898 |
| | d | 0.365 | 0.358 | 0.256 | 0.195 |
| Φ_-/Φ_+ | s | 0.862 | 0.862 | 0.854 | 0.851 |
| | p | 0.708 | 0.710 | 0.686 | 0.680 |
| | d | 0.072 | 0.062 | 0.045 | -0.028 |
| $\langle \phi_v^2 \rangle^{-1/2}$ (Ry) | s | 4.651 | 4.673 | 4.149 | 4.016 |
| | p | 6.410 | 6.451 | 5.650 | 5.494 |
| | d | 0.975 | 0.957 | 0.733 | 0.609 |

that this paramagnetic state is unstable to the formation of a ferromagnetic state [$N(E_F)I(E_F) > 1$], where we have estimated $I(E_F)$ for Pd₃Fe using the Stoner parameters from the constituents taken from the work of Gunnarsson.²² This clearly shows that Pd₃Fe is ferromagnetic.

B. Pd₃Fe: Ferromagnetic calculation

We calculated the electronic structure of Pd₃Fe with spin polarization. We used the converged paramagnetic

calculation discussed in the preceding section as our starting point. The exchange correlation potential used was the von Barth and Hedin¹³ approximation to the local spin density. The calculation was done for the experimental lattice parameter and self consistency was achieved with a mesh of 220 k points in the irreducible Brillouin zone. The potential parameters obtained for the spin polarized case are displayed in Table II. We observe that the paramagnetic values are intermediate between the spin-up and spin-down results presented in Table II. These values

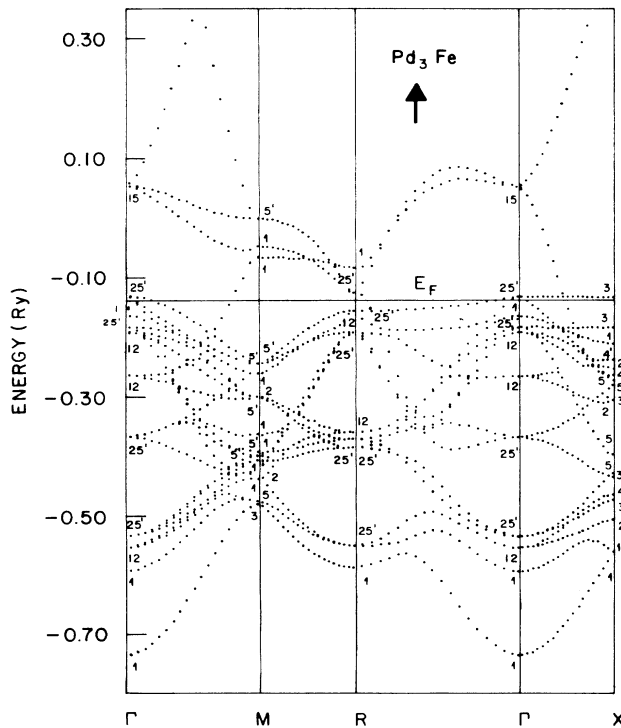


FIG. 2. Spin-up energy bands of ordered ferromagnetic Pd₃Fe along symmetry lines of the sc Brillouin zone.

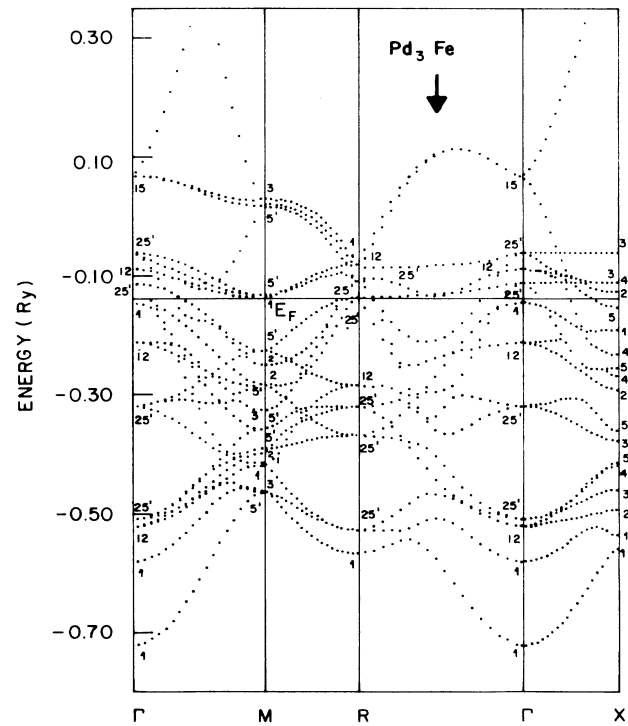


FIG. 3. Spin-down energy bands of ordered ferromagnetic Pd₃Fe along symmetry lines of the sc Brillouin zone.

TABLE III. Intrinsic masses for pure Pd and Fe and for the ordered Pd₃Fe.

| | <i>s</i> | <i>p</i> | <i>d</i> |
|------------------------------------|----------|----------|----------|
| Pd | 0.753 | 0.835 | 7.077 |
| Fe | 0.751 | 0.875 | 9.425 |
| Pd ₃ Fe (paramagnetic) | | | |
| Pd | 0.747 | 0.826 | 6.906 |
| Fe | 0.796 | 0.910 | 11.338 |
| Pd ₃ Fe (ferromagnetic) | | | |
| Pd | | | |
| ↑ | 0.747 | 0.826 | 6.896 |
| ↓ | 0.745 | 0.825 | 6.793 |
| Fe | | | |
| ↑ | 0.807 | 0.923 | 12.657 |
| ↓ | 0.790 | 0.905 | 10.637 |

differ from the previous paramagnetic calculation, reflecting the fact that spin-up and spin-down electrons feel different effective potentials. These self-consistent spin polarized potentials give the energy bands for electrons with spin up in Fig. 2 and spin down in Fig. 3, for some symmetry directions in the Brillouin zone for the simple cubic

(sc) lattice with four atoms (i.e., one Fe and three Pd atoms). We see that the spin-up bands are almost filled while the spin-down bands are partially empty. In the ΓX direction for both spin directions we see near the Fermi level some flat bands, these bands come from the folding of the XW direction of the fcc onto the sc lattice. For the spin-up electrons we have one of these flat bands very close to the Fermi energy, at -4.1 mRy from E_F . For spin-down electrons the band splitting shifts the down-spin flat bands away from E_F in the region of empty states. A flat band appears in the pure Pd and also in pure Fe. The Pd flat band in the fcc structure when folded into the sc structure of Pd₃Pd would produce a flat band quadruply degenerate. The substitution of the fourth Pd by Fe to form Pd₃Fe lifts this degeneracy, which is further split by spin polarization, as we can see in Figs. 2 and 3.

In Table III we present the intrinsic masses for the bands of pure Pd and Fe and for the intermetallic Pd₃Fe in the paramagnetic and ferromagnetic phases. We note that in the formation of the intermetallic compound (paramagnetic phase) there is a broadening of the *d* band of Pd, while the Fe bands become narrower when compared with the case of pure Pd and Fe, both calculated in the fcc phase.²¹ This indicates that in going from the pure metals to the compound the lattice spacing between Fe atoms increases, narrowing the bands, while for the Pd atoms the opposite occurs, namely, Pd atoms are closer in

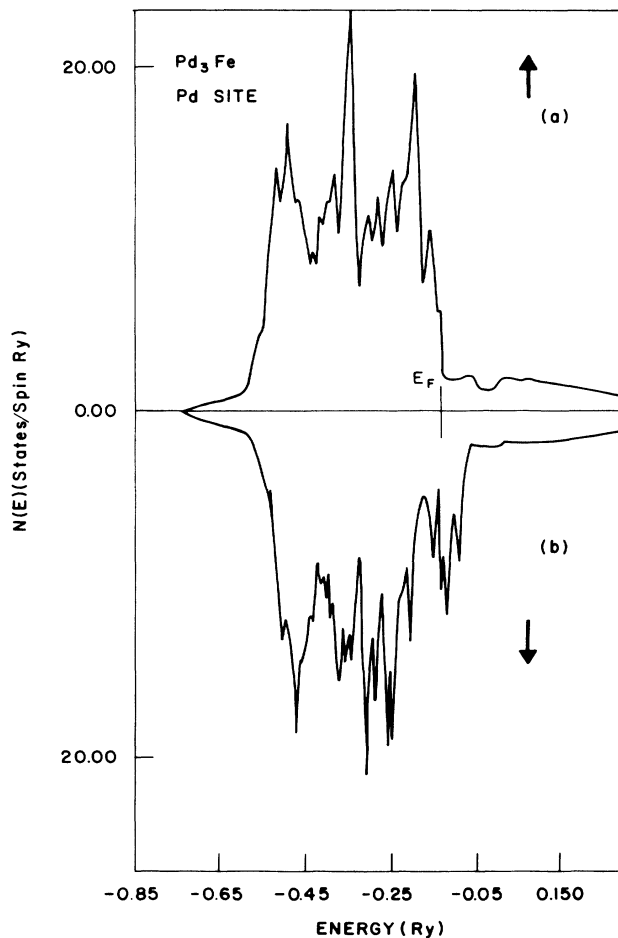


FIG. 4. Total density of states (in states/spin Ry). (a) spin-up and (b) spin-down electrons at the Pd site for Pd₃Fe.

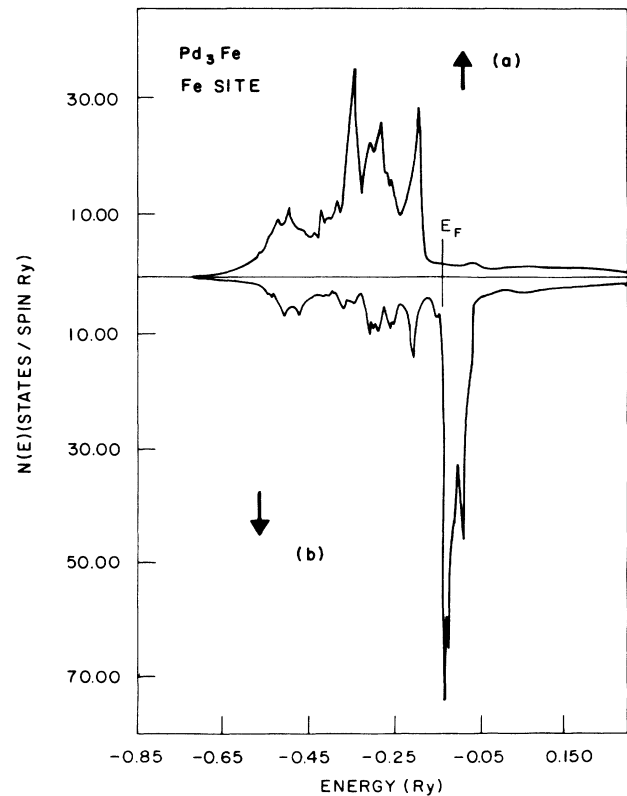


FIG. 5. Total density of states (in states/spin Ry). (a) spin-up and (b) spin-down electrons at the Fe site for Pd₃Fe.

TABLE IV. Calculated parameters for spin-polarized Pd₃Fe using the self-consistent potentials.

| | Pd | | <i>m</i> | Fe | | <i>m</i> |
|----------------------------------------------------------------|--------|--------|----------|--------|--------|----------|
| | ↓ | ↑ | ↑-↓ | ↓ | ↑ | ↑-↓ |
| <i>n</i> (electrons/spin) | 4.81 | 5.19 | 0.38 | 2.44 | 5.54 | 3.10 |
| <i>n</i> (electrons/spin) | 0.32 | 0.31 | -0.01 | 0.33 | 0.34 | 0.01 |
| <i>n</i> (electrons/spin) | 0.36 | 0.33 | -0.03 | 0.39 | 0.40 | 0.02 |
| <i>n</i> (electrons/spin) | 4.13 | 4.52 | 0.40 | 1.70 | 4.80 | 3.07 |
| <i>N</i> (<i>E_F</i>) (states/spin Ry) | 5.31 | 2.68 | | 18.47 | 2.09 | |
| <i>N_s</i> (<i>E_F</i>) (states/spin Ry) | 0.05 | 0.20 | | 0.05 | 0.26 | |
| <i>N_p</i> (<i>E_F</i>) (states/spin Ry) | 0.46 | 0.50 | | 0.25 | 0.54 | |
| <i>N_d</i> (<i>E_F</i>) (states/spin Ry) | 4.80 | 1.98 | | 18.17 | 1.29 | |
| <i>N</i> (<i>E_F</i>) (states/atom Ry) | 8.00 | | | 20.56 | | |
| <i>N</i> (<i>E_F</i>) (states/unit-cell Ry) | | | 44.56 | | | |
| γ_{theo} (mJ/mol K ²) | | | 7.61 | | | |
| | | | 4.97 | | | |
| γ_{expt} (mJ/mol K ²) | | | 8.17 | | | |
| <i>E_F</i> (Ry) | | | -0.1298 | | | |
| VMTZ (Ry) | -0.757 | -0.760 | | -0.740 | -0.737 | |

the compound than in the pure metal. In the spin-polarized case we see that spin-up electrons have narrow bands in both type of sites, which shows a localization of spin-up *d* electrons.

The states for up-spin *d* electrons are full, the contribution of these states for the DOS at *E_F* is low, which can be observed in Figs. 4 and 5 showing the DOS at the Pd and Fe sites. Previously we saw that the paramagnetic case gave us a peak for the DOS at *E_F* (Fig. 1). We see now that the spin-polarization results in a splitting of up and down bands, putting the Fermi level between the peak of the DOS of up and down spins. This reduction of *N*(*E_F*) puts it in good agreement with γ , the measured linear coefficient of the specific heat.

The general trend of ferromagnetic Pd₃Fe, as can be seen from Figs. 4 and 5, showing that electrons in this compound are as delocalized as the electrons of pure Pd and Fe, furthermore the Pd [Fig. 4(a)] and the Fe [Fig. 5(a)] spin-up electrons form a common *d* band. On the other hand, the Fe spin-down electrons are almost excluded from the Fe sites [Fig. 5(b)], which produces a localized magnetic moment at the Fe sites. The result is that we have formation of magnetic moments out of completely delocalized electrons, as observed by Kubler *et al.*²³ for Heusler alloys.

In Table IV we present some theoretical parameters obtained for Pd₃Fe with spin polarization. The contributions for the DOS at *E_F*, *N*(*E_F*), and number of electrons, *n*(*E_F*), are mainly due to the *d* electrons and the magnetization in both sites show reasonable agreement with the experiments. For the magnetic moment at the Fe site our value is greater than for the experiment, while for the magnetic moment at the Pd site the theoretical value is smaller than in the experiment. The discrepancy between our values and the experiments could be due to the use of the von Barth-Hedin approximation to the spin-density functional theory for the magnetic calculation. As we are trying to describe the competition between bonding and magnetism, a better description of correlation should be used, such as the Vosko-Wilk-Nusair²⁴

exchange-correlation energy density, since it has been shown to describe better the correlation effects at the electronic densities found in transition metals.²⁵ But perhaps it may be even necessary to go beyond the local-density approximation, that is, to include nonlocal effects, to obtain more accurate results for this alloy. The fact that we did not include spin-orbit coupling could also account for the discrepancy between theory and experiment.

The projected densities of states show that at *E_F* the *d* contribution is the most relevant. In both sites the spin-down contribution is considerable at *E_F* and the Fe spin-

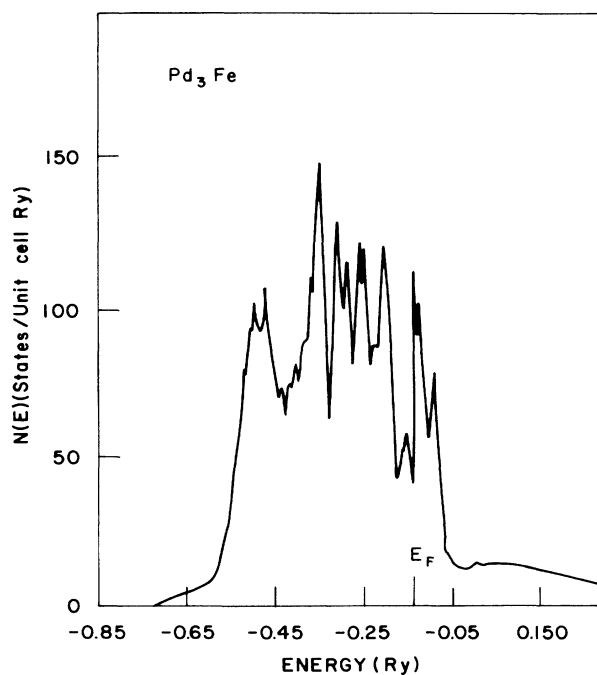


FIG. 6. Total density of states (in states/unit cell Ry) for the ordered ferromagnetic Pd₃Fe alloy (sc structure).

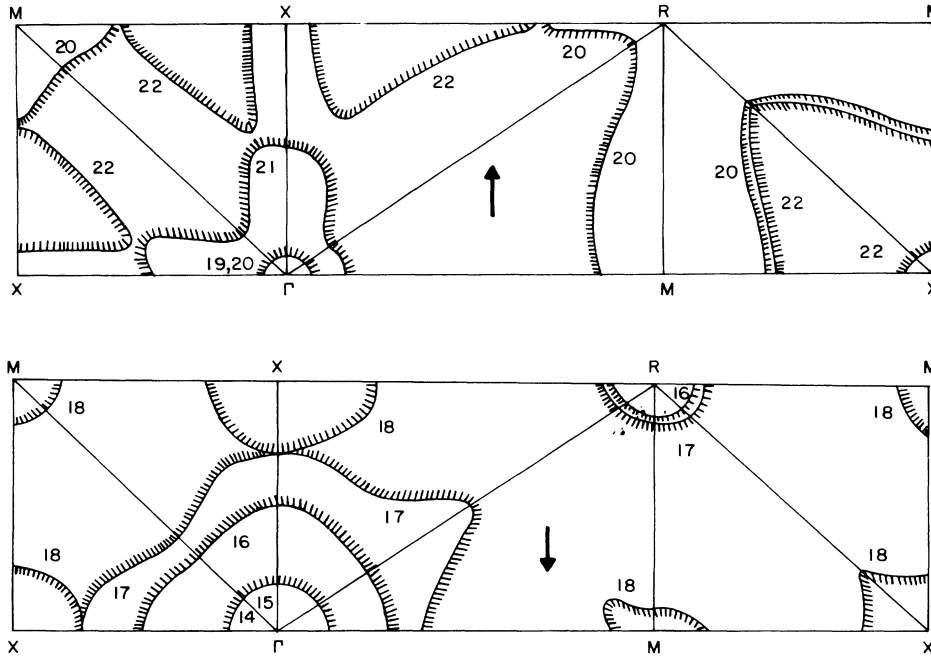


FIG. 7. Cross sections of Fermi surfaces for up and down spin for ferromagnetic Pd₃Fe by symmetry planes in the Brillouin zone. Numbers indicated the particular bands involved. Hachures on occupied side.

up contribution is very low. The total DOS at E_F show that the contribution from the Fe site is three times that of the Pd site. In Fig. 6 we show the total density of states for the ordered Pd₃Fe, in which we can see that the Fermi level is in a valley of the DOS. The total DOS per unit cell at E_F is $N(E_F) = 44.5$ states/unit-cell Ry, which gives a coefficient for the specific heat $\gamma = 7.61$ mJ/mol K² in good agreement with the experimental value as shown in Table IV. A comparison with the result of Fletcher²⁶ ($\gamma = 4.97$ mJ/mol K² for a non-self-consistent calculation) shows that self-consistency gives results in much better agreement with the experiment. The mass-enhancement factor α for the specific heat is defined by

$$\gamma = \gamma_0(1 - \alpha),$$

where γ is the experimental value for the specific-heat coefficient (in units of DOS) and $\gamma_0 = N(E_F)$ the calculated DOS. For the calculated $N(E_F)$ we estimate the mass-enhancement factor to be $\alpha = 0.0736$ while Fletcher obtained $\alpha = 0.644$. In our calculation many-body effects are considered through the exchange and correlation potential. Therefore the mass-enhancement factor includes other many-body effects like the electron-phonon interaction which we did not include explicitly.

C. Fermi surface

Figure 7 shows the intersection of the spin-polarized Fermi surface of Pd₃Fe with principal symmetry planes of the sc lattice. The Fermi surface shown in Fig. 7 has some similarities with a previous APW non-self-consistent calculation of Fletcher,²⁶ but it also shows some differences. In accordance with our previous discussion of the

value of $N(E_F)$ and its comparison with the linear coefficient of specific heat, we feel that we have a good description of the band at E_F . A surprising fact which emerges from our calculation is that there is no hole tube Fermi surface along the ΓX in either spin directions which were calculated in the similar compound Pd₃Sn,²⁷ and which was believed to be present in Pd₃Fe. Instead Fig. 7(a) shows hole tubes along the MR direction due to spin-up band 20. This is a pure Pd band which comes from the folding of the electrons Fermi surface of fcc Brillouin zone of Pd into the sc Brillouin zone of Pd₃Fe with a little distortion. To make sure that small variations in E_F do not change Fig. 7, we also calculated the Fermi surface for variations from E_F up to ± 7 mRy and we did not find any substantial changes in the Fermi surface.

The spin-up Fermi surface has a large contribution from Pd d electrons from bands 19–21. Band 22 is of d character with 70% contribution from Pd and 30% from Fe. This sheet of Fermi surface has flat portions along ΓX direction which can be connected by (100) and (110) vectors. The spin-down Fermi surface has contributions of three Pd d bands 14–16. Bands 17 and 18 are d character with 70% Fe and 30% Pd contribution, so there is a considerable contribution of Fe to the spin-down Fermi surface.

IV. DISCUSSION

In this work we used the LMTO method of Andersen to obtain the band structure of ordered spin-polarized Pd₃Fe. The theoretical results, in the form of magnetic moments and linear coefficient of specific heat, have shown good agreement with the experimental values. We

believe that the discrepancy between our results and the experiments could be due to the use of the local-density approximation, or to the fact that we did not include spin-orbit coupling. For the present discussion these results suffice to give a very good idea of the electronic structure of Pd₃Fe.

This calculation has helped us understand some questions about this interesting system, but there is still a great deal to be learned. In particular the question concerning

the disordered phase of Pd₃Fe has to be addressed if one is to get a clear understanding of this system. Questions about order-disorder transformation in this system could be considered, if we had also a calculation of the electronic structure of the disordered phase of Pd₃Fe. We are considering this very problem, which shall be subject of another publication in the near future.

We hope that the calculation presented here will be helpful to experimentalists working with Pd₃Fe.

*Permanent address: Universidade Federal de Santa Catarina, Departamento de Fisica-UFSC, Santa Catarina, Brazil.

¹C. A. Bechman, W. E. Wallace, and R. S. Craig, *Philos. Mag.* **27**, 1249 (1973).

²A. J. Smith, W. G. Stirling, and T. M. Holden, *J. Phys. F* **7**, 2411 (1977).

³G. Longworth, *Phys. Rev.* **172**, 572 (1968).

⁴A. Z. Men'shikov and V. A. Tsurin, *Phys. Met. Metallogr. (USSR)* **47**, 68 (1979); **45**, 82 (1978).

⁵T. M. Holden, *J. Phys. F* **6**, 433 (1976).

⁶M. H. P. Correa, A. Vasquez, M. I. da Costa Jr., P. J. Viccaro, and C. E. T. Goncalves da Silva, *Solid State Commun.* **40**, 211 (1981).

⁷T. B. Flanagan, S. Majchrzak, and B. Baranowski, *Philos. Mag.* **25**, 257 (1972).

⁸H. Yamada and M. Shimizu, *J. Phys. F* **7**, L203 (1977).

⁹M. H. P. Correa, A. Vasquez, and C. E. T. Goncalves da Silva, *Solid State Commun.* **42**, 251 (1982).

¹⁰P. Hohenberg and W. Kohn, *Phys. Rev.* **136**, B864 (1964).

¹¹W. Kohn and L. J. Sham, *Phys. Rev.* **140**, A1133 (1965).

¹²L. Hedin and B. I. Lundqvist, *J. Phys. C* **4**, 2064 (1971).

¹³U. von Barth and L. Hedin, *J. Phys. C* **5**, 1629 (1972).

¹⁴O. K. Andersen, *Phys. Rev. B* **12**, 3060 (1975).

¹⁵J. Korringa, *Physica* **13**, 392 (1947).

¹⁶W. Kohn and N. Rostoker, *Phys. Rev.* **94**, 1111 (1954).

¹⁷O. Jepsen, *Phys. Rev. B* **12**, 2988 (1975).

¹⁸O. Jepsen, D. Glotzel, and A. R. Mackintosh, *Phys. Rev. B* **23**, 2684 (1981).

¹⁹H. L. Skriver, *The LMTO Method: Muffin-Tin Orbitals and Electronic Structure* (Springer, New York, 1984).

²⁰O. Jepsen and O. K. Andersen, *Solid State Commun.* **9**, 1763 (1971).

²¹C. A. Kuhnen and E. Z. da Silva (unpublished).

²²O. Gunnarsson, *J. Phys. F* **6**, 587 (1976).

²³J. Kubler, A. R. Williams, and C. B. Sommers, *Phys. Rev. B* **28**, 1745 (1983).

²⁴S. H. Vosko, L. Wilk, and M. Nusair, *Can. J. Phys.* **58**, 1200 (1980).

²⁵D. Bagayoko and J. Callaway, *Phys. Rev. B* **28**, 5419 (1983).

²⁶G. C. Fletcher, *J. Magn. Magn. Mater.* **45**, 139 (1984).

²⁷H. L. Skriver, *Phys. Rev. B* **14**, 5187 (1976).